Computer Simulation Study of Human Locomotion with a Three-Dimensional Entire-Body Neuro-Musculo-Skeletal Model*
(I. Acquisition of Normal Walking)

Kazunori HASE** and Nobutoshi YAMAZAKI***

A model having a three-dimensional entire-body structure and consisting of both the neuronal system and the musculo-skeletal system was proposed to precisely simulate human walking motion. The dynamics of the human body was represented by a 14-rigid-link system and 60 muscular models. The neuronal system was represented by three sub-systems: the rhythm generator system consisting of 32 neural oscillators, the sensory feedback system, and the peripheral system expressed by static optimization. Unknown neuronal parameters were adjusted by a numerical search method using the evaluative criterion for locomotion that was defined by a hybrid between the locomotive energy efficiency and the smoothness of the muscular tensions. The model could successfully generate continuous and three-dimensional walking patterns and stabilized walking against mechanical perturbation. The walking pattern was more stable than that of the model based on dynamic optimization, and more precise than that of the previous model based on a similar neuronal system.

Key Words: Biomechanics, Human Engineering, Motion Control, Muscle and Skeleton, Computer Simulation, Walking, Neural Oscillator, Optimization

1. Introduction

The study of human walking motion has shifted from analytical studies consisting of experiments and measurements, to predictive and synthetic studies performed using computer simulations. The use of computer simulations to generate human movement not only enables *in vivo* dynamic loads, such as joint moments and muscular tensions, to be quantitatively determined, but also allows states of body motion, such as falling, to be easily realized, albeit virtually. Such realization is difficult or impossible using practical experiments. These simulation methods may be used in sports science and clinical medicine to predict the effects of training exercises or orthopedic surgery.

In previous studies, various simulation models of human bipedal walking have been extensively proposed. Such studies range from relatively simple models[1),(2)] that provide mathematical analyses to more complex or practical models that have applications in clinical medicine[3),(4)], robotics[5)] or computer graphics[6),(7)]. However, the practical application of a human walking model requires a much more precise model that is capable of three-dimensionally emulating the actual human musculo-skeletal structure. Walking patterns, such as pathological walking, often consist of three-dimensional entire-body motions, such as bilateral swing in the frontal plane and compensatory motions, including rotation of the upper body. Although three-dimensional models for walking have already been proposed[4),(8),(9)], it was difficult for some of those to keep or maintain dynamic balance during more than one walking cycle. These models could not be applied for the investigation of walking stability, such as falling in older adults. The others employed robot-like control theories as a control system without emulating that of actual human neurophysiology[5),(6)]. It is necessary for the walking model to consider not only the precise musculo-skeletal system but also the neuronal system, such as

* Received 15th April, 2002 (No. 02-4068)
** National Institute of Advanced Industrial Science and Technology, Central 6, 1-1-1 Higashi, Tsukuba, Ibaraki 305-8566, Japan. E-mail: kazunori.hase@aist.go.jp
*** Faculty of Science and Technology, Keio University, 3-14-1 Hiyoshi, Kouhoku, Yokohama, Kanagawa 223-8522, Japan

the central pattern generators (CPG) and the reflexes.

The purpose of the present study is to construct a precise simulation method for human bipedal walking that more closely emulates actual human walking, and can therefore be applied in various research fields, e.g., clinical medicine. We construct a three-dimensional bipedal walking model having a musculo-skeletal system of the entire body that includes the upper extremities. The proposed model possesses a motor control mechanism to stabilize walking patterns based on neurophysiological knowledge. We also examine a method for autonomously acquiring the human walking pattern using this model. In addition, this report is also the arrangement, extension and detailed explanation of the author's previous research[10].

2. Method

2.1 Neuro-musculo-skeletal model

In the biomechanical research field, most studies have employed dynamic optimization as a control method[1),(3),(4),(8),(9)], in which the dynamic optimization problem was converted into a parameter optimization problem with muscular activation patterns being unknown[8),(9)]. One advantage of the method is the direct access to the muscular forces required to accomplish the desired motor task or performance criteria. However, one limitation is that no somatic sensory feedback control is included as in human reflexes. Therefore, the model based on dynamic optimization sufficiently simulates ballistic movement, such as jumping; however, it is difficult to simulate non-ballistic and stable movement, such as continuous walking against mechanical perturbation.

Meanwhile, Taga and coworkers[11)–(13)] simulated human walking motion based on the hypothesis that bipedal walking is generated when a rhythm pattern formed by the neuronal system cooperates mutually with a pendulum-like rhythm pattern produced by the body's dynamic system. These models could perform stable walking in unstable environments, such as slopes, and under mechanical disturbance. The present authors[14)] have also developed a two-dimensional walking model based on Taga's hypothesis. In the present study, the theory described above was adopted as the basic mechanism for motor control, and the resulting model is referred to as the neuro-musculo-skeletal model. The neuro-musculo-skeletal model was composed of the rigid link system, the muscular geometry system and the neuronal system with neural oscillators and sensory feedback paths included. Figure 1 is a diagram denoting the control system of the neuro-musculo-skeletal model. The outline of the model is described below. See the Appendix section for the details.

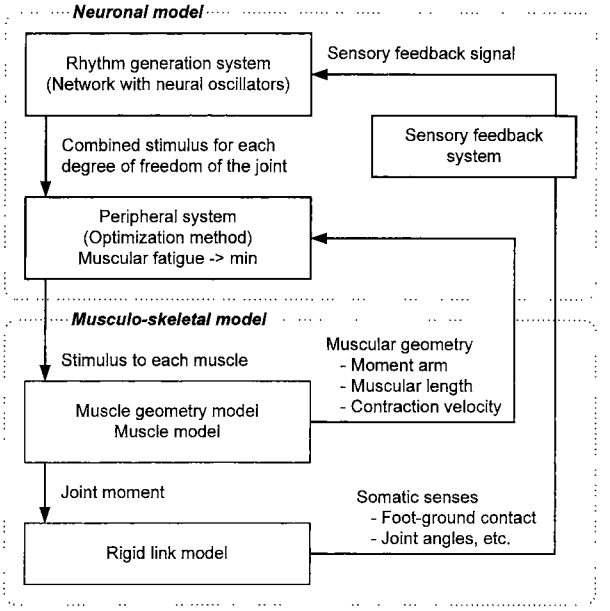

Fig. 1 An outline of the control system of the neuro-musculo-skeletal model

2.2 Rigid link model

The inertial properties of the entire human body are represented by a three-dimensional 14-rigid-link system. These links include the feet, the calves, the thighs, the pelvis, the lower part of the lumbar spine, the upper part of the lumbar spine, the thorax including the head and neck, the upper arms, and the forearms, as shown in Figs. 2 and 3. The trunk segment was divided into four parts in order to simply represent spinal curvature. The hip and lower lumbar joints have three rotational degrees of freedom and all other joints have one degree of freedom. A visco-elastic passive moment induced by soft tissues was assumed to act on the joint. The interaction between foot and ground was modeled as a combination of springs and dampers. The ground reaction forces produced by springs and dampers were assumed to act on four points in each foot: two points in the heel and two points in the toe of the foot. The inertial properties of each body segment, such as mass and moment of inertia, were determined from previous literature[15),(16)]. The proposed model assumed the subject to be 1.75 m tall and to weigh 68 kg.

2.3 Muscle geometry model

In order to represent the anatomical arrangements of muscles in the human body, a muscular geometry model consisting of 60 muscles for the entire body was constructed, as shown in Fig. 2. The geometry of each muscular arrangement was represented by a series of line segments. The series of line segments connected the insertion, the origin and a couple of 'via points' of the muscle. Each point was fixed in the

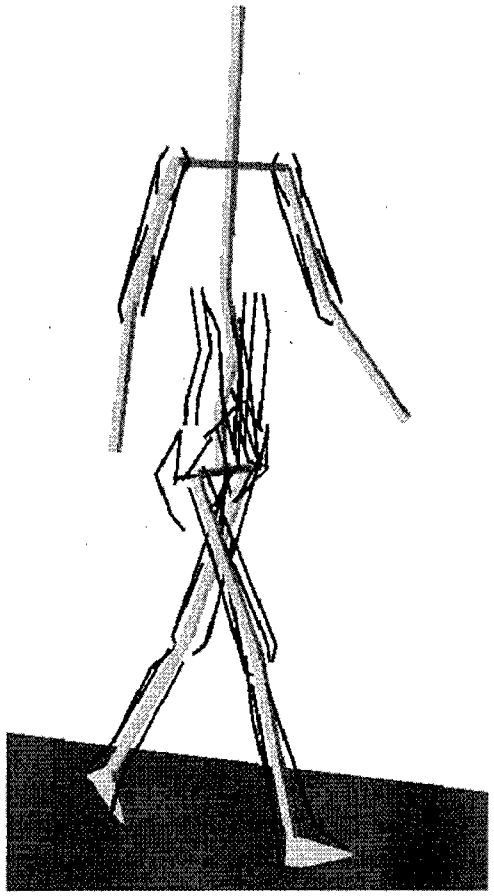

Fig. 2 Three-dimensional model of the musculo-skeletal system. The shaded thin boxes abstractly represent the rigid link system of the entire body. The bold lines indicate the muscle geometry models represented by a series of line segments.

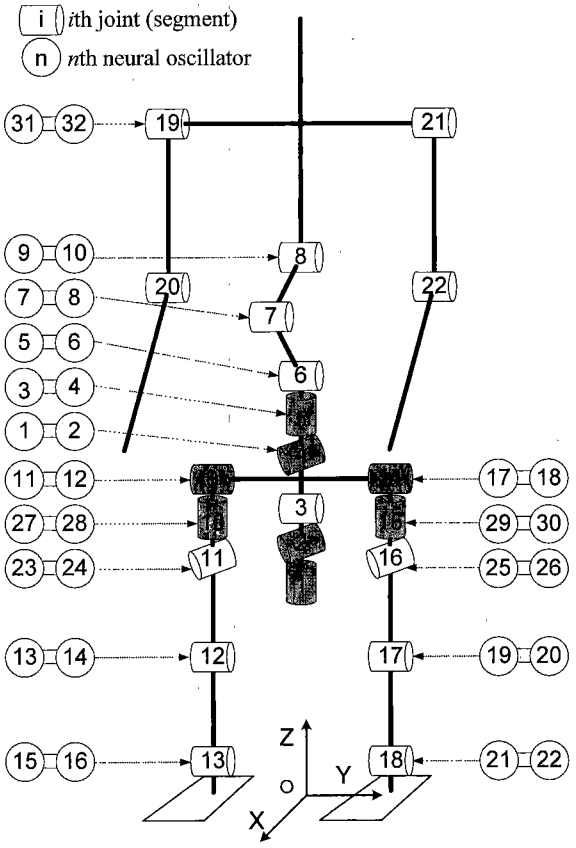

Fig. 3 Definition of the multi-rigid-link system in the body dynamics and the neural oscillators. The cylinder model represents a pin joint with one degree of freedom of rotation. The number in the cylinder model represents the segment number (i.e., joint number) defined. The circles denote the neural oscillators. See the Appendix section for the details.

appropriate segment coordinate system. Therefore, the moment arm of the muscle changes according to the joint angles. Each muscle exerts its force in response to stimuli from the neuronal system, driving the body model expressed by the multi-rigid-link system. Equations of the length-force and velocity-force relationships[17] were considered in the mechanical properties of the muscular model.

2.4 Neuronal model

The functions of the neuronal system were divided into three types, as shown in Fig. 1. The first neuronal sub-system is a rhythm generation system corresponding to the spinal cord level. This neuronal system represents a rhythm generation mechanism with central pattern generators (CPGs)[18], and was modeled as a recurrent network system consisting of neural oscillators[19]. This generates the neuronal stimulus by receiving a nonspecific stimulus from the higher center and feedback signals from the sensory feedback system. Each neural oscillator is mathematically expressed by two differential equations. Figure 3 indicates the relationship between the neural oscillators and the degrees of freedom of the joints. A pair of the neuron exists for each degree of freedom of the joint, so that the output from the neural oscillator represents the neuronal stimulus combined for the degree of freedom. However, both the shoulder joints are controlled by one pair of neurons and no neuron exists for the elbow joints to simplify the model. The neuronal system model consists of 32 neural oscillators in total.

The second neuronal model represents a sensory feedback system approximately corresponding to the reflexes. This consisted of complex algebraic equations as shown in the Appendix section. These equations were determined after referring to previous literature[11),(12)] and muscular activity patterns estimated by electromyograms and inverse dynamics model[20]. The system receives the somatic senses, such as the angular displacements of the joints and the body segments, the angular velocity of those, foot-

ground contacts, and the center of gravity of the entire body, and sends the feedback signals to the neural oscillators.

The third is a neuronal system corresponding to the peripheral level. The neuronal system divides the combined neuronal stimulus from the neural oscillator into the neuronal stimulus to each muscle. The model corresponds to a macroscopic model of reciprocal innervation. The model was mathematically represented as a static optimization problem. That is, optimization calculations were performed under the following conditions: unknown parameters for the neuronal stimuli to the muscles; equality conditions for the equilibrium equations between muscular tensions and joint moments; inequality conditions for positive neuronal stimulus values; and objective function expressed as a minimizing mechanism for muscular fatigue[21]. The calculation of muscular tension is affected by changes in the moment arm, length and contraction velocity of the muscle. The static optimizations were performed for the five muscular groups of the four extremities and the trunk part independently at each time interval for numerical solution of the differential equations of motion.

2.5 Mathematical expression

In this nonlinear, nonequilibrium system, it is expected that bipedal walking can be generated through the mutual entrainment between the nonlinear dynamics of the neuronal system and the musculo-skeletal system[11],[12]. From the models mentioned above, we can derive a total of 114 nonlinear, first-order differential equations: 50 equations of motion for the body dynamical system and 64 equations for the neuronal system. Mathematically, the walking pattern is generated by solving all the differential equations simultaneously.

2.6 Acquisition of walking pattern

In the neuronal model, many parameters must be determined. We have proposed a numerical search method to determine the parameters using the criteria for evaluating walking motion and genetic algorithms for optimization techniques[14]. In the present study, this search method was used in an attempt to determine the parameters of the neuronal system.

The calculations were performed as described below.

(1) Walking motion is generated by numerically solving the differential equations of the neuro-musculo-skeletal system from the initial conditions.

(2) The criterion for evaluating the motion pattern is calculated based on the generated walking motion.

(3) The parameters of the neuronal system are adjusted infinitesimally to improve the evaluative criterion for walking.

(4) The above process is repeated until there is no apparent improvement of the evaluative criterion.

In case that walking motion is generated, the initial conditions for motion, such as joint angles and joint angular velocities, are necessary to numerically solve the differential equations. In the search process, when the walking pattern was generated, the kinematic data in the middle of the continuous walking were picked up by which the initial conditions of the next step for the repeated calculation were defined. That is, the initial conditions were variable as the search calculation proceeded and the simulated walking pattern was assumed to be steady.

Because the number of the neuronal parameters was too many to be determined by only the search method, several parameters were assumed to be constant, and a number of relationships among parameters were assumed as proportional in order to reduce the number of search parameters in the actual calculation. In total, 125 parameters of the neuronal system were adopted as unknown search parameters. See the Appendix section for the neuronal parameters to be searched.

2.7 Evaluative criterion for normal walking

Various motion patterns can be synthesized by determining a proper evaluative criterion for locomotion. In the present study, an evaluative criterion for normal walking was decided under the following consideration.

It is thought from the previous studies that the criteria for human movement are classified into the following two types. One is related to locomotive energy efficiency. Experiments on actual human walking have revealed that normal walking patterns in humans are determined to minimize energy consumption in the entire body per unit locomotive distance[22]. The criterion is equivalent to an index called the *specific power* that evaluates a vehicle's price speed[23]. Many papers have also discussed the criteria based on the energy efficiency[8],[9],[24]. Another of the criteria is related with the smoothness of movement. Many studies have reported that human movement, such as that of reaching by the upper extremity, was determined to maximize the smoothness, such as the muscular tensions[25], joint moments[26] and jerk of kinematical data[27].

From our previous experimental study[24], we thought that the energy efficiency was the first principle for human locomotion. However, there was still a small gap between minimum-energy walking pattern in theory and normal walking pattern in actual humans, so that we thought that another supplementary criterion, such as motion smoothness mentioned

the above, was necessary to fill the gap. According to these thoughts, a hybrid criterion between the energy efficiency and the motion smoothness was employed in the present study as the evaluative criterion for normal walking as follows:

$$C=1/(S+\omega D) \rightarrow \max, \quad (1)$$

where C is the evaluative criterion, S is the specific power, ω is the weighting coefficient and D is the rate of change of the muscular tensions. In this hybrid criterion, an index for energy efficiency was formulated by the specific power and an index for motion smoothness was formulated by the rate of change of the muscular tensions. The specific power and the rate of change of the muscular tensions should be minimized so that the reciprocal was employed in the criterion. The specific power and the rate of change of the muscular tensions were expressed as follows:

$$S=\frac{\int\left(\sum_m \dot{E}_m+\dot{B}\right)dt}{gMD_{istance}}, \quad (2)$$

$$D=\frac{\int\sum_m(\dot{F}_m/A_m)^2dt}{P_{eriod}}, \quad (3)$$

where $\dot{E}_m$ is the energy consumption rate in the mth muscle, $\dot{B}$ is the energy consumption rate in regions other than muscles (e.g., internal organs), M is the body mass, g is the acceleration of gravity, $D_{istance}$ is the traveling distance, $\dot{F}_m$ is the mth muscular tension rate, A_m is the physiological cross sectional area of the mth muscle and P_{eriod} is the period of time spending in walking. See the Appendix section for the detailed calculation of the energy consumption in the muscles and in the internal organs. It was expected that a normal walking pattern would be generated by adjusting the neuronal parameters to maximize the above criterion.

2.8 Implementation

All programs were written in C language on a Linux operating system, and the improved Euler method was used for numerical solution of differential equations. The step-size of time was set as 0.4 ms. In the numerical search process to achieve the normal walking pattern desired, 10 000 iterations were conducted. Genetic algorithms were employed as the computing technique of the numerical search. Six steps of walking were performed in each repeated calculation. The calculation took about 12 hours using a PC cluster system consisting of 34 CPUs (TAKERU2000; NABE International, Inc., Japan).

3. Results

3.1 Acquisition of normal walking

Figure 4 indicates the walking patterns achieved by the simulation. At the beginning of the search process, the model generated a walking pattern with unstable steps. As the search proceeded, a more efficient and smoother walking pattern was obtained around the 10 000th repeated calculation. At the final stage, the specific power and the rate of change of muscular tensions were improved by 26% and 103% respectively compared with the initial stage.

3.2 Stable walking

The simulation model could walk continuously more than 50 steps, if the differential equations for the neuro-musculo-skeletal model were solved without a break. Figure 5 shows the phase plane described by combinations of the angles and angular velocities in the hip, knee and ankle joints for 50 steps of walking. The orbit was not steady, but settled in a certain width.

To demonstrate walking stability, an external force was added to the pelvis segment during continuous walking. As shown in Fig. 6, the model could walk continuously against mechanical perturbation without falling.

3.3 Kinematic and dynamic data for walking

Figure 7 shows the kinematic and dynamic data obtained from the simulation results, such as the joint angles, the ground reaction forces, the joint moments and the muscular tensions during one walking cycle. Because the proposed model included sufficient musculo-skeletal detail, various *in vivo* loads and kinematic data were obtained quantitatively, as shown in the figure. The data presented are from walking at a walking speed of 1.39 m/s, a stride length of 1.52 m, a step width of 0.20 m, and a walking cycle time of 1.09 s.

In general, the simulated walking pattern agrees closely with that of an actual human. For example, it was found that the vertical ground reaction force has

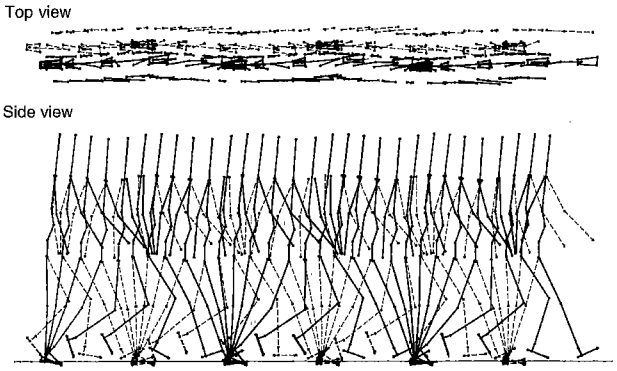

Fig. 4 Simulated walking patterns. For the top and side views, six-step walking patterns are continuously illustrated. Each stick picture is traced at 0.1 s intervals. The upper and lower extremities of the right side are represented by solid lines, and those of the left side are represented by broken lines.

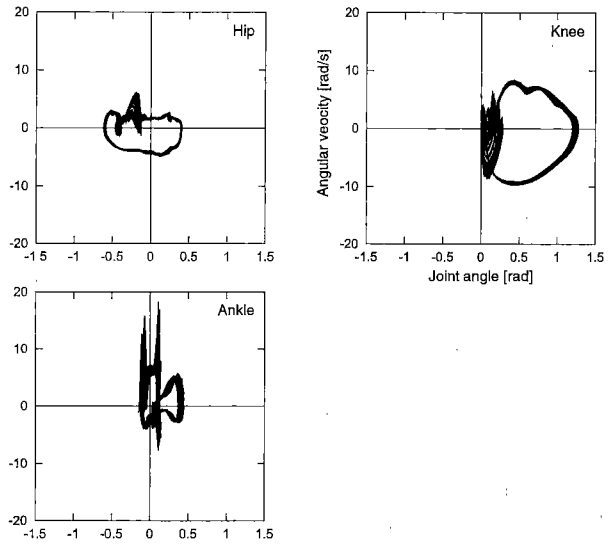

Fig. 5 Phase planes of combinations between the angles and angular velocities in the hip, knee and ankle joints for 50 steps of walking

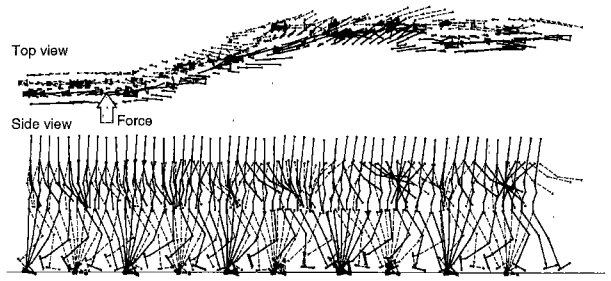

Fig. 6 An example of walking pattern when an external force of 80 N acted on the pelvis segment in the mediolateral direction for 0.2 s

a two-peak waveform, which is one of the characteristics in normal walking. Basic cadence parameters, such as walking speed, were also found to correspond well to those of average human gait. However, some differences between the simulation results and actual human walking motion were also observed. For example, the extensor moment on the hip joint was relatively higher and the extensor moment on the knee joint during the stance phase was lower than those of an actual human[20].

4. Discussion

4.1 Evaluation of model and walking pattern

The proposed simulation method has the following characteristics: the body dynamic system and the musculo-skeletal system were represented three-dimensionally; the entire body including the upper extremities and the spinal curvature was modeled; the neuronal system was expressed by mathematical elements, such as neural oscillators, sensory feedback paths and an optimization problem, corresponding to

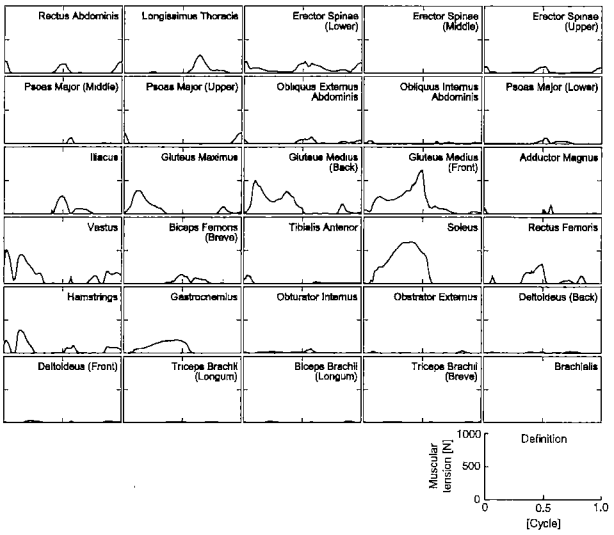

(a) Muscular tensions

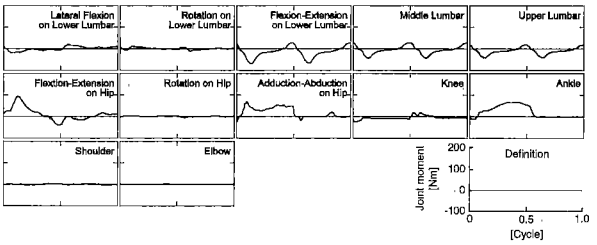

(b) Joint moments

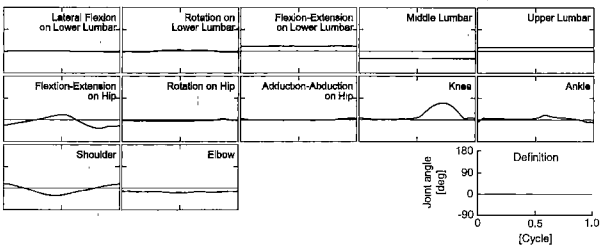

(c) Joint angles

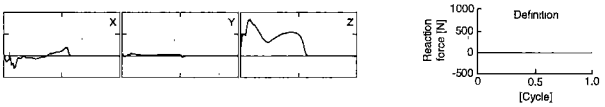

(d) Ground reaction forces

Fig. 7 Kinematical and dynamic data obtained from the simulation results. (a) Muscular tensions, (b) Joint moments, (c) Joint angles, (d) Ground reaction forces. For all the graphs, time is normalized by the time for one walking cycle: 0 and 1 indicate when the right heel touches the ground. For the muscular tensions and ground reaction forces, the data related with the right side of the body were illustrated. For the joint moments and angles, the data with respect to the left upper and lower extremities were omitted. The positive values of the joint moment and angle show clockwise movements.

the actual neuronal system to some degree; the neuronal parameters were autonomously adjusted using the numerical search method; the model could generate a three-dimensional continuous walking pattern stabilized against a mechanical perturbation; not only kinematic data but also *in vivo* dynamic data, such as muscular tensions and energy consumption, were quantitatively obtained using the model.

Compared with previous simulation models, these characteristics are significant for a simulation technique. Methods of generating bipedal walking have been developed in several fields, such as robotics and computer graphics, especially for three-dimensional motion. In robotics, many studies have attempted to generate bipedal walking using computer simulation and even actual hardware[5],[28]. However, few models exist that are capable of realizing walking speed and walking patterns that are similar to actual human gait. Moreover, control rules of bipedal walking are generally created as an application of modern control theory and are not always used to simulate actual motor control mechanisms in humans. Computer graphics have been used to generate more natural and complicated walking[6],[7] and even running motions[29]; however, such walking does not usually reflect the dynamical and physiological properties of the body. Many methods depend on the skill of computer-graphic operators and the measurement of motion data. In the field of biomechanics, using relatively simple models, bipedal walking has been analyzed both theoretically and mathematically with respect to stability[1],[2]. However, these models are designed for specific purposes and provide little if any versatility. Recently, a precise three-dimensional walking model has been proposed[8],[9]; however, the model was of controlled dynamic optimization without feedback control, and could walk during only one or half a walking cycle. Although Taga and coworkers' locomotion model[11]–[13] has successfully synthesized stable walking to keep a dynamic balance against mechanical perturbation, the model was two-dimensional, and the motion pattern did not consider evaluative criteria, such as the specific power and muscular smoothness.

In contrast, the proposed model in the present study has the characteristics mentioned above. We also believe that the model validity is sufficient to investigate global characteristics for walking, such as stability and efficiency. Many factors of the neuro-musculo-skeletal system involved with actual human gait were considered in the model; therefore, the proposed model is expected to enable simulation of more diversified and complicated patterns. This simulation model provides excellent versatility and practicability, and it should be useful in research in which the relationship between biomechanical properties of the body and the motion patterns must be precisely investigated, such as in clinical medicine.

4.2 Problems to be solved

In the proposed search method, major alterations of the neuronal parameters were performed primarily by human trial and error, rather than by a computer. Parameters had to be adjusted by trial and error in order for the walking model to walk the initial few steps. Therefore, the proposed search method cannot always completely determine the parameters. In addition, the structure of the neuronal system itself, especially the sensory feedback system, was determined not only by referring to neurophysiological knowledge, but also by referring to biomechanical measured data of gait, such as the joint angles and moments. The developmental process of the neuronal model was very time consuming. The ultimate problem to be solved is that not only neuronal parameters but also the structure of the neuronal system itself are determined autonomously based on neurophysiological knowledge. That is, the neuronal system of gait simulation should model more precisely mechanical properties of the nervous system, such as the muscle spindle and Golgi tendon organ[30]. A method of determining the neuronal parameters by a mathematical, computational approach could also be an effective means of reducing the time and effort involved in trial and error analysis by humans[31]. We must investigate the problem from both computational and neurophysiological points of view.

We believe that the simulation results, such as for the walking pattern, were highly valid from a macroscopic point of view. However, if waveforms of each muscular tension and joint angle were looked at from a microscopic point of view, differences between the simulation results and actual human walking motion were found. It is also necessary to modify the simulation model in field of biomechanics and neurophysiology.

5. Conclusions

In order to improve the practicability of the simulations of human bipedal walking, a model that more precisely simulates the human body structure for the neuro-musculo-skeletal system was developed. Neuronal parameters were adjusted using the numerical search method to improve the evaluative criterion for locomotion defined by a hybrid between the specific power and the rate of change of the muscular tensions. As a result, three-dimensional and stable walking that corresponds well to actual human walking motion was synthesized.

From an engineering point of view, a simulation study should use a simpler model to aid ease of analysis. However, the simpler model has hardly been accepted from a practical point of view, such as for clinical medicine. The proposed model of the present study corresponds with actual humans in terms of the body structure and generated motion. Therefore, it is expected that the model will be applied in various practical research fields, such as clinical medicine.

Acknowledgments

The authors gratefully acknowledge the contributions of S. E. Halliday, A. B. Zavatsky, and B. J. Andrews. We would like to thank Drs. A. J. "Knoek" van Soest and M. F. Bobbert for their stimulating discussions.

Appendix: Expressions of the Neuro-Musculo-Skeletal Model

A. 1 Coordinate system

The multi-rigid-link system representing the human body structure was defined as shown in Fig. 3. Each segment was mathematically defined to connect with the next segment through a pin joint with one rotational degree of freedom. A joint having more than two degrees of freedom, such as the hip joint, was represented using the combination of the imaginary segments with zero weight and zero length. Therefore, there is a one-to-one correspondence between the joint and the segment. The joint numbers (i.e., segment numbers) were defined as shown in Fig. 3. The number 1, 2 and 3 segments are such imaginary segments to represent rotational degrees of freedom existing between the multi-rigid-link system and the absolute-coordinates system. Because the imaginary segments are included in the multi-rigid-link system, the number of segments is 22 in the actual calculation while the number of segments is 14 in the model of the musculo-skeletal system. Regarding the global-coordinates system, the origin was located on the ground, the X axis corresponds with the anteroposterior direction of walking movement, the Y axis corresponds with the mediolateral direction, and the Z axis corresponds with the vertical axis, as shown in Fig. 3.

A. 2 Equations of motion for the rigid link model

As for the derivation of the equations of motion, the method described by Walker and Orin[32] was expanded. A systematic method that is applicable to a multi-link system having branched structures, such as the entire body (including the extremities), and no fixed point was developed. A similar derivation method for the equation of motion is described by Fujimoto and Kawamura[28].

The model has 22 rotational degrees of freedom and three translational degrees of freedom. In general, the equations of motion were expressed as follows:

$$\boldsymbol{M}(\boldsymbol{q})\ddot{\boldsymbol{q}}+\boldsymbol{h}(\boldsymbol{q},\dot{\boldsymbol{q}})=\boldsymbol{n} \tag{A1}$$

where $\boldsymbol{q}=[q_1, q_2,\cdots, q_i,\cdots, q_{22}, q_x, q_y, q_z]^T$ is a 25×1 state variable vector of the motion, $q_1, q_2,\cdots, q_i,\cdots, q_{22}$ are the ith joint angles, q_x, q_y, q_z are the displacements of the origin of the multi-link system (i.e., the origin of the pelvis segment), $\boldsymbol{n}=[n_1, n_2,\cdots, n_i,\cdots, n_{22}, 0, 0, 0]^T$ is a 25×1 vector related with driving forces, $n_1, n_2,\cdots, n_i,\cdots, n_{22}$ are the ith gross joint moments (including passive joint moments), $\boldsymbol{M}$ is a 25×25 inertial matrix and $\boldsymbol{h}$ is a 25×1 vector related with external forces, Coriolis forces and gravity. $\boldsymbol{M}$ and $\boldsymbol{h}$ are derived from the derivation method for the equations of motion.

A. 3 Joint moment

The passive element of the joint was assumed to exist on each degree of freedom, independently. It was described as the following nonlinear function as in the literature[1].

$$n_{Pi}=-\kappa_{i1}\exp(-\kappa_{i2}(q_i-\kappa_{i3}))+\kappa_{i4}\exp(-\kappa_{i5}(\kappa_{i6}-q_i))+\kappa_{i7}\dot{q}_i \tag{A2}$$

where n_{Pi} is the passive moment of the ith joint, and $\kappa_{i1}, \kappa_{i2}, \kappa_{i3}, \kappa_{i4}, \kappa_{i5}, \kappa_{i6}, \kappa_{i7}$ are the coefficients. The gross joint moment n_i was explained by the sum of the passive moment n_{Pi} and the muscular moment caused by the muscular tensions n_{Mi} as follows:

$$n_i=n_{Mi}+n_{Pi}. \tag{A3}$$

A. 4 Ground reaction forces

The ground reaction forces acting on the four points for each foot were expressed as follows:

if $h_{zj}<0$

$$G_{xj}=-\xi_1(h_{xj}-h_{0xj})-\xi_2\dot{h}_{xj}$$
$$G_{yj}=-\xi_1(h_{yj}-h_{0yj})-\xi_2\dot{h}_{yj}$$
$$G_{zj}=-\xi_1(h_{zj}-0)+\xi_2\max(-\dot{h}_{zj}, 0)$$

otherwise

$$G_{xj}=G_{yj}=G_{zj}=0 \tag{A4}$$

where G_{xj}, G_{yj}, G_{zj} are three-dimensional ground reaction forces for the jth point of application, h_{xj}, h_{yj}, h_{zj} denote the position of the jth point of application, h_{0x_j}, h_{0y_j} denote the rest position of the spring that is reset to the point at which the point first contact the ground, and ξ_1, ξ_2 are the elastic and viscous coefficients ($\xi_1=9\,000$ [N/m], $\xi_2=400$ [Ns/m]).

A. 5 Muscular model

Each muscle model has the mechanical properties of the force-velocity relationship and the force-length relationship expressed by the following expression[17]:

$$F_m=A_m\eta f_L(l_m)f_V(l_m, v_m)s_m$$
$$f_L(l_m)=0.32+0.71\exp(-1.112(l_m-1))\times\sin(3.722(l_m-0.656))$$
$$f_V(l_m, v_m)=(1+\tanh(3.0v_m))/0.99$$

$$-0.01\exp(-2.6(l_m-1))$$
$$l_m=l_m/\bar{L}_m$$
$$v_m=\dot{L}_m/V_{MAX} \tag{A5}$$

where F_m is the mth muscular tension, A_m is the physiological cross-sectional area (PCSA) of the muscle, η is the coefficient representing the maximum muscular tension per unit PCSA ($\eta=5\cdot10^5$ [N/m^2]), $f_L(\cdot)$ is the force-length relationship, $f_V(\cdot)$ is the force-velocity relationship, L_m is the muscle length, $\bar{L}_m$ is the natural resting length of the muscle, l_m is the muscle length normalized by its natural resting length, V_{MAX} is the maximum contraction velocity of the muscle, v_m is the muscular contraction velocity normalized by its maximum contraction velocity, and s_m is the normalized neuronal stimulus given from the neuronal model. The natural resting length of the muscle $\bar{L}_m$ was simply defined as the muscle length at the static standing posture. The maximum contraction velocity of the muscle V_{MAX} was assumed constant by 5.0 m/s for all the muscles.

A. 6 Rhythm generation system

Figure 3 also shows the connection of neural oscillators and their correspondence with the multi-link system. The dynamics of each neural oscillator were expressed as the following differential equations[11),(12),(19)]:

$$\tau_n\dot{u}_n=-u_n+\sum_{\tilde{n}}\delta_{n\tilde{n}}\max(u_{\tilde{n}},0)-\beta z_n+u_0+f_{eed_n}(\boldsymbol{q},\dot{\boldsymbol{q}})$$
$$\tau_n'\dot{z}_n=-z_n+\max(u_n,0) \tag{A6}$$

where u_n is the inner state of the nth neural oscillator, z_n is the state variable representing the fatigue of the neural oscillator, τ_n, τ_n' are the time constants, $\delta_{n\tilde{n}}$ is the weight of the interconnection between neural oscillators, β is the fatigue constant, u_0 is the nonspecific stimulus from the higher centre, such as the mesencephalic locomotor region (MLR), and $f_{eed_n}(\boldsymbol{q},\dot{\boldsymbol{q}})$ is the sensory feedback signal from the sensory feedback system.

The output from the neural oscillators was changed into the combined stimuli by using the following simple equation:

$$c_i=\sum_n\lambda_{in}\max(u_n,0) \tag{A7}$$

where c_i is the neuronal stimulus combined for each degree of freedom of the ith joint and λ_{in} is the weighting coefficient.

A. 7 Sensory feedback system

Sensory feedback system to neural oscillators was represented as shown below.

$$f_{eed_1}=-\alpha_1q_4-\alpha_2\dot{q}_4-\alpha_3(\theta_{x6}+\theta_{x7}+\theta_{x8})-\alpha_4(\dot{\theta}_{x6}+\dot{\theta}_{x7}+\dot{\theta}_{x8})-\alpha_5(c_{ogy}-q_y)-\alpha_6\dot{c}_{ogy}$$
$$f_{eed_3}=-\alpha_7(q_5+0.1\dot{q}_5)+\alpha_8(g_r-g_l)+\alpha_9(\theta_{z3}+0.1\dot{\theta}_{z3})-\alpha_{10}(\theta_{z8}+0.1\dot{\theta}_{z8})$$
$$f_{eed_5}=\alpha_{11}(\theta_{y6}-\bar{\theta}_{y6})+\alpha_{12}\dot{\theta}_6+\alpha_{13}(q_{y6}-\bar{q}_6)+\alpha_{14}\dot{q}_6$$
$$f_{eed_7}=\alpha_{15}(\theta_{y7}-\bar{\theta}_{y7})+\alpha_{16}\dot{\theta}_{y7}+\alpha_{17}(q_7-\bar{q}_7)+\alpha_{18}\dot{q}_7$$
$$f_{eed_9}=\alpha_{19}(\theta_{y8}-\bar{\theta}_{y8})+\alpha_{20}\dot{\theta}_{y8}+\alpha_{21}(q_8-\bar{q}_8)+\alpha_{22}\dot{q}_8$$
$$f_{eed_{11}}=\alpha_{23}(\theta_{y11}+\alpha_{24})^3-\alpha_{25}(\theta_{y16}+\alpha_{24})^3+\alpha_{26}\theta_{y12}g_r-\alpha_{27}g_r-\alpha_{28}(\theta_{y3}-\bar{\theta}_{y3})g_r-\alpha_{29}(\theta_{y3}-\bar{\theta}_{y3})(1-g_r)-\alpha_{30}\dot{\theta}_{y3}g_r-\alpha_{31}\dot{\theta}_{y3}(1-g_r)$$
$$f_{eed_{13}}=-\alpha_{32}\theta_{y11}u_{nit}((1-g_r)+g_l)+\alpha_{33}\theta_{y17}u_{nit}((1-g_r)+g_l)-\alpha_{34}(\theta_{y11}+\alpha_{35})^3(1-g_r)+\alpha_{36}q_{12}g_r+\alpha_{37}(g_r-g_rg_lu_{nit}(p_{x18}-p_{x13}))$$
$$f_{eed_{15}}=-\alpha_{38}\theta_{y11}g_r-\alpha_{39}\theta_{y12}g_r-\alpha_{40}\theta_{y12}{}^3g_r+\alpha_{41}(\dot{\theta}_{x13}-\dot{\theta}_{x12})g_r-\alpha_{42}g_r+\alpha_{43}(1-g_r)$$
$$f_{eed_{17}}=\alpha_{23}(\theta_{y16}+\alpha_{24})^3-\alpha_{25}(\theta_{y11}+\alpha_{24})^3+\alpha_{26}\theta_{y17}g_l-\alpha_{27}g_l-\alpha_{28}(\theta_{y3}-\bar{\theta}_{y3})g_l-\alpha_{29}(\theta_{y3}-\bar{\theta}_{y3})(1-g_l)-\alpha_{30}\dot{\theta}_{y3}g_l-\alpha_{31}\dot{\theta}_{y3}(1-g_l)$$
$$f_{eed_{19}}=-\alpha_{32}\theta_{y16}u_{nit}((1-g_l)+g_r)+\alpha_{33}\theta_{y12}u_{nit}((1-g_l)+g_r)-\alpha_{34}(\theta_{y16}+\alpha_{35})^3(1-g_l)+\alpha_{36}q_{17}g_l+\alpha_{37}(g_l-g_rg_lu_{nit}(p_{x13}-p_{x18}))$$
$$f_{eed_{21}}=-\alpha_{38}\theta_{y16}g_l-\alpha_{39}\theta_{y17}g_l-\alpha_{40}\theta_{y17}{}^3g_l+\alpha_{41}(\dot{\theta}_{x18}-\dot{\theta}_{x17})g_l-\alpha_{42}g_l+\alpha_{43}(1-g_l)$$
$$f_{eed_{23}}=-\alpha_{44}\theta_{x3}g_r-\alpha_{45}\dot{\theta}_{x3}g_r+\alpha_{46}(g_r-g_rg_l)+\{-\alpha_{47}(c_{ogy}-p_{y13}-\alpha_{48})+\alpha_{49}\dot{p}_{y12}-\alpha_{50}\dot{c}_{ogy}\}\times(1-g_r)\max(p_{x12}-p_{x10},0)$$
$$f_{eed_{25}}=\alpha_{44}\theta_{x3}g_l+\alpha_{45}\dot{\theta}_{x3}g_l+\alpha_{46}(g_l-g_rg_l)+\{-\alpha_{47}(p_{y18}-c_{ogy}-\alpha_{48})-\alpha_{49}\dot{p}_{y18}+\alpha_{50}\dot{c}_{ogy}\}\times(1-g_l)\max(p_{x18}-p_{x16},0)$$
$$f_{eed_{27}}=-\alpha_{51}(\theta_{z13}+0.1\dot{\theta}_{z13})(1-g_r)\max(p_{x13}-p_{x11},0)-\alpha_{52}(\theta_{z3}+0.1\dot{\theta}_{z3})g_r$$
$$f_{eed_{29}}=-\alpha_{51}(\theta_{z18}+0.1\dot{\theta}_{z18})(1-g_l)\max(p_{x18}-p_{x16},0)-\alpha_{52}(\theta_{z3}+0.1\dot{\theta}_{z3})g_l$$
$$f_{eed_{31}}=\alpha_{53}(\theta_{y19}{}^3-\theta_{y21}{}^3)+\alpha_{54}(g_r-g_l)+\alpha_{55}(\theta_{z8}+q_1+0.2\dot{\theta}_{z8}+0.2\dot{q}_1)$$
$$f_{eed_n}=-f_{eed_{n-1}}\quad(n=2,4,6,\cdots,30,32)$$
$$f_{eed_{elbow\_R}}=-\alpha_{56}(q_{20}+\alpha_{57}+0.1\dot{q}_{20})$$
$$f_{eed_{elbow\_L}}=-\alpha_{56}(q_{22}+\alpha_{57}+0.1\dot{q}_{22}) \tag{A8}$$

where $\dot{q}_i$ is the ith joint angle, θ_{xi}, θ_{yi}, θ_{zi} denote the absolute angle of the ith link segment from each absolute coordinates axis, $\bar{q}_{yi}$, $\bar{\theta}_{yi}$ are the neutral angles at the static standing posture, c_{ogx}, c_{ogy}, c_{ogz} denote the position of the centre of gravity for all body segments, p_{xi}, p_{yi}, p_{zi} denote the displacement of the origin of the ith link segment, g_r is the on-off signal which takes a value of 1 when the right foot is on the ground and a value of 0 when the right foot is off the ground, g_l is similarly the on-off signal for the left foot, $u_{nit}(x)$ is the function taking on a value of 1 if $x>0$ and 0 otherwise, and α_1, α_2,$\cdots$, α_{57} are the coefficients. $f_{eed_{elbow\_R}}$, $f_{eed_{elbow\_L}}$ denote the feedback signals for the right and left elbow joints, and are transformed into the combined neuronal stimuli c_i for the elbow joints without neural oscillators.

These equations were determined after referring to previous literature[11),(12)] and muscular activity patterns estimated by electromyograms and inverse dynamics model[20)]. These equations were basically

based on the following rule, though there are some exceptions:

[feedback signal]=Σ[gate signal]×[gain signal]
[gate signal]=$gate(g_r, g_l, u_{nit}(x))$
[gain signal]=$gain$([angular displacement]
−[offset angular displacement]
+[coefficient]×[angular velocity]) (A9)

Almost all of the gain function, $gain(x)$, is defined as a simple linear function, such as $gain(x)=x$; however, some feedback signal is defined using a nonlinear gain function, such as $gain(x)=x^3$, in order to gain the amplitude.

A. 8 Neuronal peripheral system

The calculation conditions of the optimization method to determine each neural stimulus to each muscle were as follows:

Variables: s_m

Object function: $J=\sum_m s_m{}^3 \rightarrow \min$

Constraints: $s_m \geq 0$

$$c_i=\sum_m r_{im}F_m \quad \text{(A10)}$$

where r_{im} is the moment arm of the mth muscle on the ith joint that was defined by the muscle geometry model.

A. 9 Neuronal parameters

In the above equation for the neuronal system, τ_n, τ_n', $\delta_{n\tilde{n}}$, β, u_0, α_1, $\alpha_2,\cdots,\alpha_{57}$, and λ_{in} are the neuronal parameters to be determined. By assuming the symmetry of the neuronal model, 22 coefficients in τ_n were employed as the search parameters, as well as τ_n' and λ_{in}. $\delta_{n\tilde{n}}$ is assumed constant. β, u_0, α_1, $\alpha_2,\cdots,\alpha_{57}$ were also employed. Therefore, a total of 125 parameters of the neuronal system were adopted as unknown search parameters.

A. 10 Energy consumption in the muscle

Energy consumption in each muscle was explained as in the literature[33] as follows:

$$\dot{E}_m=\dot{E}_{Am}+\dot{E}_{Mm}+\dot{E}_{Sm}+\dot{E}_{Wm}$$
$$\dot{E}_{Am}=\varepsilon_A w_m s_m$$
$$\dot{E}_{Mm}=\varepsilon_M w_m f_L(l_m) s_m$$
$$\dot{E}_{Sm}=\begin{cases}-\dot{L}_m \varepsilon_S A_m \eta f_L(l_m) s_m & \dot{L}_m<0\\ 0 & \dot{L}_m \geq 0\end{cases}$$
$$\dot{E}_{Wm}=\begin{cases}-\dot{L}_m F_m & \dot{L}_m<0\\ 0 & \dot{L}_m \geq 0\end{cases} \quad \text{(A11)}$$

where $\dot{E}_{Am}$ is the muscle activation heat rate, $\dot{E}_{Mm}$ is the muscle maintenance heat rate, $\dot{E}_{Sm}$ is the muscle shortening heat rate, $\dot{E}_{Wm}$ is the muscle mechanical work rate, ε_A is the coefficient of the muscle activation heat ($\varepsilon_A=0.1$), ε_M is the coefficient of the muscle maintenance heat ($\varepsilon_A=40.0$), and ε_S is the coefficient of the muscle shortening heat ($\varepsilon_S=0.25$). w_m is the muscular mass given by the following simple equation:

$$w_m=A_m \bar{L}_m \rho \quad \text{(A12)}$$

where ρ is the muscular density ($\rho=1\,050\ \mathrm{kg/m^3}$)

A. 11 Energy consumption in the viscera

The energy consumption rate, excluding that of muscles $\dot{B}$[W] was assumed to be the energy rate of basal metabolism in the body and was calculated using the following regression equation[24], where M is body weight in kg.

$$\dot{B}=0.685M+29.8 \quad \text{(A13)}$$

References

(1) Davy, D.T. and Audu, M.L., A Dynamic Optimization Technique for Predicting Muscle Forces in the Swing Phase of Gait, Journal of Biomechanics, Vol. 20 (1987), pp. 187-201.

(2) Garcia, M., Chatterjee, A., Ruina, A. and Coleman, M., The Simplest Walking Model: Stability, Complexity, and Scaling, ASME Journal of Biomechanical Engineering, Vol. 120 (1998), pp. 281-288.

(3) Yamaguchi, G.T. and Zajac, F.E., Restoring Unassisted Natural Gait to Paraplegics via Functional Neuromuscular Stimulation: A Computer Simulation Study, IEEE Transactions on Biomedical Engineering, Vol. BME-37 (1990), pp. 886-902.

(4) Tashman, S., Zajac, F. E. and Perkash, I., Modeling and Simulation of Paraplegic Ambulation in a Reciprocating Gait Orthosis, ASME Journal of Biomechanical Engineering, Vol. 117 (1995), pp. 300-308.

(5) Hirai, K., Hirose, M., Haikawa, Y. and Takenaka, T., The Development of the Honda Humanoid Robot, Proceedings of IEEE Conference on Robotics and Automation, (1998), pp. 1321-1326.

(6) Laszlo, J., van de Panne, M. and Fiume, E., Limit Cycle Control and Its Application to the Animation of Balancing and Walking, SIGGRAPH 96 Conference Proceedings, (1996), pp. 155-162.

(7) Sun, H.C. and Metaxas, D.N., Automating Gait Generation, SIGGRAPH 2001 Conference Proceedings, (2001), pp. 261-269.

(8) Anderson, F.C. and Pandy, M.G., Static and Dynamic Optimization Solutions for Gait Are Practically Equivalent, Journal of Biomechanics, Vol. 34 (2001), pp. 153-161.

(9) Anderson, F.C. and Pandy, M.G., Dynamic Optimization of Human Walking, ASME Journal of Biomechanical Engineering, Vol. 123 (2001), pp. 381-390.

(10) Hase, K., Nishiguchi, J. and Yamazaki, N., Model of Human Walking with Three-Dimensional Musculo-Skeletal System and Hierarchical Neuronal System, Biomechanism 15, the Society of Biomechanism (ed.), (in Japanese), (2000), pp. 187-198, University of Tokyo Press, Tokyo.

(11) Taga, G., Yamaguchi, Y. and Shimizu, H., Self-Organized Control of Bipedal Locomotion by Neural Oscillators in Unpredictable Environment, Biological Cybernetics, Vol. 65 (1991), pp. 147-159.

(12) Taga, G., A Model of the Neuro-Musculo-Skeletal System for Human Locomotion I, Emergence of Basic Gait, Biological Cybernetics, Vol. 73 (1995), pp. 97-111.
(13) Taga, G., A Model of the Neuro-Musculo-Skeletal System for Human Locomotion II, Real-Time Adaptability under Various Constraints, Biological Cybernetics, Vol. 73 (1995), pp. 113-121.
(14) Yamazaki, N., Hase, K., Ogihara, N. and Hayamizu, N., Biomechanical Analysis of the Development of Infant Walking by the Neuro-Musculo-Skeletal Model, Folia Primatologica, Vol. 66 (1996), pp. 253-271.
(15) Chandler, R.F., Clauser, C.E., McConville, J.T., Reynolds, H.M. and Young, J.W., Investigation of Inertial Properties of the Human Body, AMRL-TR-74-137, (1975), Wright-Patterson Air Force Base, Ohio.
(16) Zatsiorsky, V. and Seluyanov, V., The Mass and Inertia Characteristics of the Main Segments of the Human Body, Biomechanics VIII-B, Matsui, H. and Kobayashi, K.(eds.), (1983), pp. 1152-1159, Human Kinetics Publishers, Champaign.
(17) Hatze, H., A Myocybernetic Control Model of Skeletal Muscle, Biological Cybernetics, Vol. 25 (1977), pp. 103-119.
(18) Grillner, S., Neurobiological Bases of Rhythmic Motor Acts in Vertebrates, Science, Vol. 228 (1985), pp. 143-149.
(19) Matsuoka, K., Sustained Oscillations Generated by Mutually Inhibiting Neurons with Adaptation, Biological Cybernetics, Vol. 52 (1985), pp. 367-376.
(20) Hase, K. and Yamazaki, N., Development of Three-Dimensional Whole Body Musculoskeletal Model for Various Motion Analyses, JSME Int. J., Ser. C, Vol. 40, No. 1 (1997), pp. 25-32.
(21) Crowninshield, R.D. and Brand, R.A., A Physiologically Based Criterion of Muscle Force Prediction in Locomotion, Journal of Biomechanics, Vol. 14 (1981), pp. 793-801.
(22) Ralston, H.J., Energetics of Human Walking, Neural Control of Locomotion, Herman, R.M., Grillner, S., Stein, P.S.G. and Stuart, D.G.(eds.), (1976), pp. 77-98, Plenum Press, New York.
(23) Gabrielli, G. and von Karman, T., What Price Speed?: Specific Power Required for Propulsion of Vehicles, Mechanical Engineering, Vol. 72 (1950), pp. 775-781.
(24) Yamazaki, N. and Hase, K., Biomechanical Criteria for Determination of Cadence and Stride Length in Free Walking, Biomechanism 11, the Society of Biomechanism (ed.), (in Japanese), (1992), pp. 179-190, University of Tokyo Press, Tokyo.
(25) Pandy, M.G., Garner, B.A. and Anderson, F.C., Optimal Control of Non-Ballistic Muscular Movements: A Constraint-Based Performance Criterion for Rising from a Chair, ASME Journal of Biomechanical Engineering, Vol. 117 (1995), pp. 15-26.
(26) Uno, Y., Kawato, M. and Suzuki, R., Formation and Control of Optimal Trajectory in Human Multijoint Arm Movement, Minimum Torque-Charge Model, Biological Cybernetics, Vol. 61 (1989), pp. 89-101.
(27) Flash, T. and Hogan, N., The Coordination of Arm Movements: An Experimentally Confirmed Mathematical Model, Journal of Neuroscience, Vol. 5 (1985), pp. 1688-1703.
(28) Fujimoto, Y. and Kawamura, A., Three Dimensional Digital Simulation and Autonomous Walking Control for Eight-Axis Biped Robot, Proceedings of IEEE International Conference on Robotics and Automation, (1995), pp. 2877-2884.
(29) Hodgins, J.K., Simulation of Human Running, Proceedings of IEEE International Conference on Robotics and Automation, (1994), pp. 1320-1325.
(30) Ogihara, N. and Yamazaki, N., Generation of Human Bipedal Locomotion by a Bio-Mimetic Neuro-Musculo-Skeletal Model, Biological Cybernetics, Vol. 84 (2001), pp. 1-11.
(31) Ok, S., Miyashita, K. and Hase, K., Evolving Bipedal Locomotion with Genetic Programming —A Preliminary Report—, Proceedings of Congress on Evolutionary Computation, (2001), pp. 1025-1032.
(32) Walker, M.W. and Orin, D.E., Efficient Dynamic Computer Simulation of Robotic Mechanisms, ASME Journal of Dynamic Systems, Measurement, and Control, Vol. 104 (1982), pp. 205-211.
(33) Hatze, H. and Buys, J.D., Energy-Optimal Controls in the Mammalian Neuromuscular System, Biological Cybernetics, Vol. 27 (1977), pp. 9-20.